Mon. Not. R. Astron. Soc. **337,** 869–874 (2002)

Chandra imaging spectroscopy of 1E 1740.7−2942

E. Gallo★ and R. P. Fender

Astronomical Institute 'Anton Pannekoek', University of Amsterdam and Centre for High Energy Astrophysics, Kruislaan 403, 1098 SJ, Amsterdam, the Netherlands

Accepted 2002 August 6. Received 2002 July 25; in original form 2002 March 13

ABSTRACT

In 2000 August, we observed the black hole candidate 1E 1740.7−2942, the brightest persistent hard X-ray source within a few degrees of the Galactic Centre, for 10 ks with *Chandra* (ACIS-I). Attempting to compensate for pile-up effects, we found that the spectra were well-fitted by an absorbed power law, with photon indices $\Gamma = 1.54^{+0.42}_{-0.37}$ (readout streak) and $\Gamma = 1.42^{+0.14}_{-0.14}$ (annulus), consistent with a black hole low/hard state. We have analysed a public observation performed by *Chandra* which utilized short frames in order to avoid severe pile-up effects. Subtracting the core point spread function from the whole image, we did not find evidence for any elongated feature perpendicular to the radio jet axis, as reported in a recent analysis of the same data. Moreover, comparing the radial profiles with those of an unscattered X-ray point source, we found an indication of an extended, previously undetected, X-ray scattering halo. The measured halo fractional intensity at 3 keV is between 30 and 40 per cent within 40 arcsec but drops below detectable levels at 5 keV. Finally, by placing a limit on the X-ray flux from the radio-emitting lobe, which has been identified as the hotspot at the end of the northern jet of 1E 1740.7−2942, we are able to constrain the magnetic energy density in that region.

Key words: binaries: general – stars: individual: 1E 1740.7–2942 – dust, extinction – X-rays: general.

1 INTRODUCTION

The black hole candidate (BHC) 1E 1740.7−2942 is the brightest hard X-ray source close to the centre of our Galaxy, with a hard X-ray spectrum and luminosity comparable to Cygnus X-1 (Liang & Nolan 1984; Sunyaev et al. 1991a; Liang 1993). Interest in this source has increased following the discovery of its association with a double-sided radio-emitting jet by Mirabel et al. (1992), since when it has been classified as a '*microquasar*'. Unfortunately 1E 1740.7−2942 suffers from extremely high galactic extinction; intense searches, both in the optical and IR bands, have failed to identify a counterpart (Prince & Skinner 1991; Mereghetti et al. 1992; Djorgovski et al. 1992; Mirabel & Duc 1992; Marti et al. 2000; Eikenberry et al. 2001). It has been proposed that 1E 1740.7−2942 is accreting from a nearby molecular cloud in which the source is likely to be embedded (Bally & Leventhal 1991; Mirabel et al. 1991; Phillips, Joseph & Lazio 1995; Yan & Dalgarno 1997). Recently, Smith, Heindl & Swank (2001) have reported on the detection of a weak periodic modulation in the long-term X-ray light curve; a period of about 12.5 d has been estimated. In addition, much effort has been devoted to the possible identification of 1E 1740.7−2942 with a source of 511-keV annihilation radiation, but no definitive confirmation has been reported so far (Bouchet et al. 1991; Sunyaev et al. 1991b; Anantharamaiah et al. 1993; Jung et al. 1995). As a result of its very high hydrogen column density ($N_{\rm H} \sim 10^{23}$ cm^{-2} – see, for example, Sheth et al. 1996; Churazov, Gilfanov & Sunyaev 1996; Sakano et al. 1999) this object is in principle an ideal candidate for investigating the properties of the X-ray scattering haloes, which are known to be generated by dust grains along the line of sight and which provide a unique opportunity to probe the dust component of the interstellar medium (see Predehl & Schmitt 1995) as well as potentially to measure the distance (Predehl et al. 2000). X-ray haloes have been observed by *Einstein, ROSAT* and *ASCA* but, thanks to the angular and energy resolution of *Chandra*, it is now possible to detect and investigate them in far greater detail than ever before. More recently, Cui et al. (2001) have observed 1E 1740.7−2942 with the high-energy transmission grating spectrometer (HETGS) of *Chandra*. They have reported on the detection of an elongated X-ray feature in the zeroth-order image, with an extension of about 3 arcsec, orientated roughly perpendicular to the radio-jet axis.

This paper is structured as follows. In Section 2 we describe the observation and we present our results. We focus on the spectral analysis and on the overall structure of the source, which has been reconstructed both from our observation and from another public observation (see Cui et al. 2001), in which the effects of the pile-up do not distort the central region of the image. In Section 3 we show some preliminary results on the X-ray halo investigation, comparing the radial profiles of 1E 1740.7−2942 with those of an X-ray point-like source, which is supposed to be unscattered. In the fourth section, we provide an estimate of the X-ray and radio fluxes coming from the radio-emitting region, which has been identified as the

★E-mail: egallo@science.uva.nl

hotspot at the end of the northern jet of 1E 1740.7−2942. The final section is devoted to our summary and conclusions.

2 OBSERVATION AND DATA ANALYSIS

We observed 1E 1740.7−2942 with the *Chandra* advanced CCD Imaging Spectrometer (ACIS; Garmire 1997) on 2000 August 30 16:59–20:00 with the nominal frame time of 3.2 s, for a total on-source time of about 10 ks. Standard processing of the data was performed by the *Chandra* X-ray Center (CXC). The Chandra interactive analysis of observations (CIAO) tools (version 2.2) together with XSPEC (version 11.1) have been used for analysing the data. The ACIS-I camera consists of an array of four front-illuminated CCDs. The physical pixel size is 0.24 μm, which at the aim-point of the telescope is comparable to the 0.5 arcsec spatial resolving power of the High-Resolution Mirror Assembly (HRMA). Each CCD contains 1024 × 1024 pixels organized into four readout nodes, each of which reads out 1024 rows and 256 columns of pixels. The source was positioned close to the aim-point of the telescope, which is about 960 rows away from the readout node, on ACIS-I device I3. As expected, because of the relatively high luminosity of 1E 1740.7−2942, the image suffers from severe pile-up effects, which affect especially the central region, giving rise to an apparent 'hole' of no events at the centre of the source. This means that the total energy of the events is larger than the threshold (∼15 keV) and is then rejected. In addition, the 'readout streak' is clearly visible, which arises because all pixels in the column, in which the bright source lies, are exposed to that source for 40 μs. The measured count rate for a circular region with a radius of four pixels centred on 1E 1740.7−2942 is 0.053 count s^{-1}. Note that, based on previous observations of 1E 1740.7−2942, PIMMS predicts a pile-up fraction for *Chandra* ACIS-I of ∼75 per cent.

2.1 X-ray spectrum

Despite the poor statistics, we have been able to extract the spectrum from the readout streak, which does not suffer from pile-up effects as a result of shorter exposure by about 80 times. In order to do this, we isolated a region with a width of five pixels [the point spread function (PSF) full width at half-maximum was about two pixels], centred on the readout streak, extending from just outside the core region to the edge of the CCD. The result is shown in Fig. 1(left panel). The best-fitting model (χ^2/d.o.f. = 82/80) requires an absorbed power law with a photon index $\Gamma = 1.54^{+0.42}_{-0.37}$. The hydrogen column density turns out to be extremely high, even for a source located in the Galactic Centre: $N_{\rm H} = 11.8^{+2.3}_{-1.9} \times 10^{22}$ cm^{-2}. The integrated unabsorbed 2–10 keV flux is 4.6×10^{-11} erg cm^{-2} s^{-1}, corresponding to an unabsorbed soft X-ray luminosity of 4×10^{34} erg s^{-1}, at a distance of 8.5 kpc. An alternative approach, delivering more counts but possibly more vulnerable to pile-up effects, is to take the X-ray spectrum from an annulus about the piled-up core. In this case, we have extracted the spectrum from an annulus between 4 and 30 arcsec (Fig. 1(right panel)). The best-fitting parameters are $\Gamma = 1.42^{+0.14}_{-0.14}$ for $N_{\rm H} = 10.45^{+0.73}_{-0.70} \times 10^{22}$ cm^{-2} with χ^2/d.o.f. = 430/331, i.e. consistent with those obtained from the readout streak. We do not believe that scattering in the dust halo, reported in Section 3, will significantly affect this spectral analysis, as the strongest scattering will occur at energies which are heavily absorbed. Our analysis is consistent with a black hole low/hard state, in agreement with Main et al. (1999), who performed a long-term monitoring of 1E 1740.7−2942; the source was observed 77 times over a period of 1000 days, and its photon index varied between about 1.4 and 1.8. Note that other recent papers (Sakano et al. 1999; Cui et al. 2001), however, have reported rather harder spectra than expected for the low/hard X-ray state, with $0.9 \leqslant \Gamma \leqslant 1.3$.

2.2 Morphology

Cui et al. (2001) have observed 1E 1740.7−2942 for about 10 ks with the *Chandra* HETGS (Observation Identity 94) adopting an alternating exposure data mode, with three long frames (nominal 3.2-s readout time) and one short (readout time of 0.3 s) in order to mitigate pile-up. Inspecting the zeroth-order image, they found evidence of an elongated X-ray feature, with an extent of about 3 arcsec, roughly perpendicular to the axis of the radio lobes. In order to establish the reality of this structure, they ran MARX simulations for the HETGS zeroth-order image of a point source and they fitted the simulated PSF to the short frame radial profile, collapsed along the elongation of such a feature. Based on this approach, they estimated that the measured profile is not point-like at a confidence level of 99.9 per cent.

In Fig. 2 we show our ACIS-I image of 1E 1740.7−2942, smoothed with a 4-arcsec Gaussian; we do not see any asymmetry in the X-ray emission on scales of a few arcmin. However, these

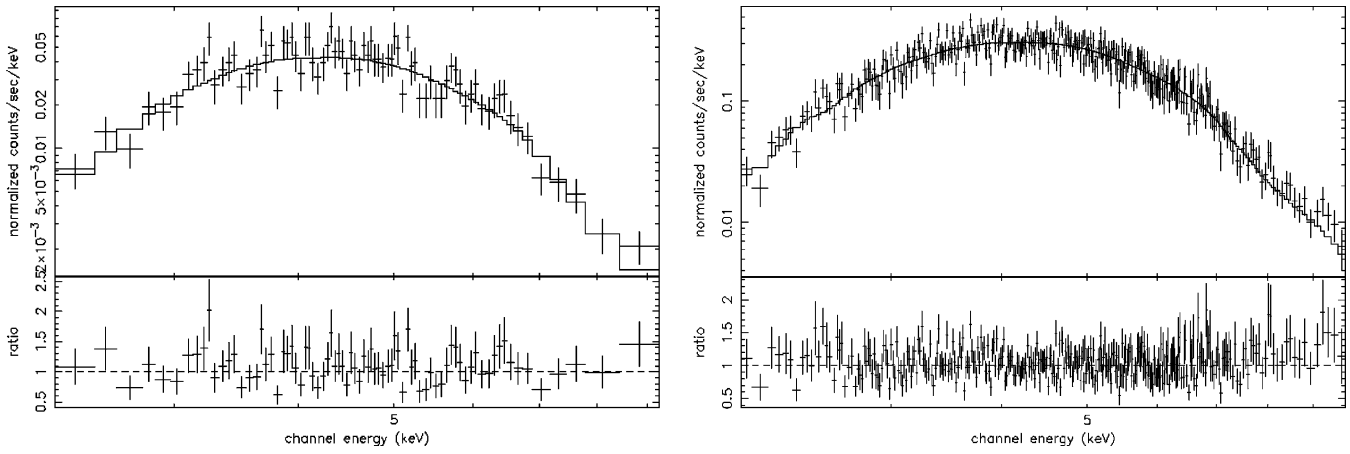

Figure 1. (Left panel) The 2–10 keV energy spectrum of 1E 1740.7−2942 extracted from the readout streak. This is well fitted by an absorbed power law with $\Gamma = 1.54^{+0.42}_{-0.37}$, $N_{\rm H} = 11.8^{+2.3}_{-1.9} \times 10^{22}$ cm^{-2} and χ^2/d.o.f. = 82/80. (Right panel) The 2–10 keV spectrum extracted from an annulus region with an internal radius of 4 arcsec. In this case we obtained $\Gamma = 1.42^{+0.14}_{-0.14}$ and $N_{\rm H} = 10.45^{+0.73}_{-0.70} \times 10^{22}$ cm^{-2} with χ^2/d.o.f. = 430/331.

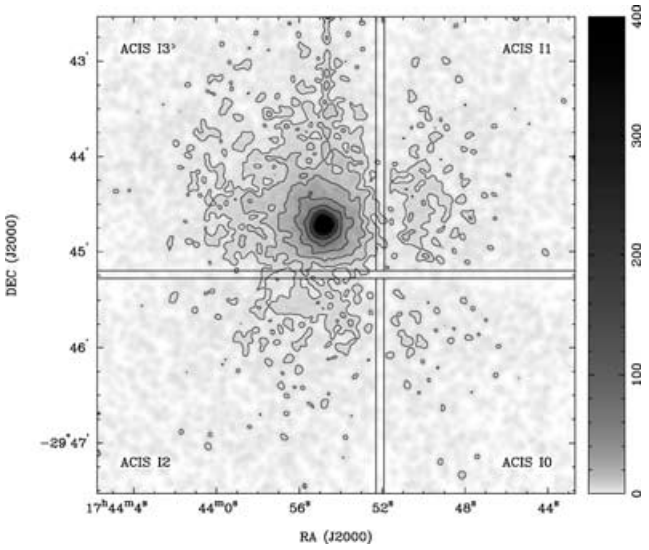

Figure 2. Our 10-ks ACIS-I image of 1E 1740.7−2942, smoothed with a 4-arcsec Gaussian. There is no evidence for asymmetric structures on arcmin-scales. The cross-like structure is a result of gaps between the chips in the ACIS-I array. Clearly visible is the readout trace, extending north, while the lack of photons in the centre does not appear because of the smoothing.

data are not useful for investigating the elongated feature reported by Cui et al. (2001), because of the aforementioned pile-up effects. Nevertheless, we have also looked at the data of Cui et al. (2001), now publicly available, by using a quite different approach, as follows. The CIAO package tool MKPSF performs an interpolation between the PSF library files, which consist of two-dimensional simulated monochromatic PSF images, stored in multi-dimensional FITS '*hypercubes*' with energies ranging from 0.277 to 8.6 keV and azimuth/elevation steps of either 1 or 5 arcmin. We extracted the *Chandra* PSF in the brightest point of the image at 5.5 keV, where the energy histogram of the short frame image reaches its maximum. Then we normalized the PSF we obtained to the total number of counts of the source and subtracted it from the short frame image of 1E 1740.7−2942, in order to identify some excess.

The result is shown in Fig. 3; a simple visual inspection of the PSF (Fig. 3, centre panel) suggests that the apparent east–west (EW) elongation could be an artefact because it appears in the PSF image itself. This conclusion is confirmed by the subtraction (Fig. 3, right panel), which does not reveal the presence of any significant asymmetry. The visible residuals appear to be a result of the fact that the normalized PSF, which is of course energy-dependent, has been calculated at 5.5 keV, where the short frame image shows its maximum in the number of counts versus energy plot. Furthermore, our experience with observations of unscattered point sources (see later) suggests that the genuine wings of the PSF are even broader than those of the library PSFs.

3 X-RAY HALO

It is well known that sufficiently dense dust clouds along the line of sight to a bright X-ray source are expected to produce haloes of faint and diffuse high-energy emission because of the (small-angle) scattering of the primary radiation by cosmic dust grains. Our goal was to extract the radial profiles of 1E 1740.7−2942 in different energy bands and to compare them to the *Chandra* PSF in order to identify any X-ray excess. Following the CIAO threads, we decided to use annuli from 3 to 100 arcsec with 2-arcsec binning, while an annulus from 100 to 110 arcsec was used for the background region. As a first step, we compared the measured profile with that of the *Chandra* PSF we obtained through an interpolation of library PSFs, as explained in the previous section. However, these library PSFs have not been derived from on-orbit calibration information; a detailed comparison of observations is still incomplete. There are indications that the shape of the library PSFs do not match the real data very well. In particular, the wings (for distances in excess of about 10 arcsec), which result mainly from scattering from the microroughness on the X-ray optic surfaces, seem to be quite different.[1] Following the same path described in the preceding section, we generated the *Chandra* PSF, by interpolation of library files, in the centre of our image. Then we extracted the PSF radial profile and normalized it to 1E 1740.7−2942 at a radial distance of 4 arcsec (∼8 pixels) (a radial distance at which pile-up effects are negligible). The slope of the PSF radial profile generated in this way is quite steep compared to the data; if fitted by a simple power-law model, the profile of the PSF (in count s^{-1} $pixel^{-1}$ versus pixel) has a $\Gamma = 3.2 \pm 0.1$ power law, while the profile of 1E 1740.7−2942 is well fitted by a $\Gamma = 2.8 \pm 0.1$ power law.

In order to rule out the suspicion that such a discrepancy was not the result of an underestimation of the PSF wings, we decided to use as a point-like source a public *Chandra* observation of the high Galactic latitude active galactic nucleus PKS 2155−304 (Observation Identity 3167). Predehl & Schmitt (1995), who performed a very accurate study on X-ray haloes around 25 point sources observed by *ROSAT*, have identified this object as an unscattered X-ray point source.

Our aim was to obtain the radial profile of this source in units of count s^{-1} $arcsec^{-2}$ versus arcsec and, again, to compare it to the 1E 1740.7−2942 profile. We calculated the surface brightness distributions using 50 annuli from 0.5 to 125 arcsec (1–300 pixel). Because of the severe pile-up effects in our observation of 1E 1740.7−2942, the comparison between the two profiles is strongly sensitive to the normalization factor. As we did before, we chose to normalize them to the measured surface brightness distribution value at about 4 arcsec, i.e. in a region where the amount of lost and undetected events should be negligible. In Fig. 4 we show the results of our halo analysis in the two representative energy bands: 2.5–3.5 keV and 4.5–5.5 keV. Clearly distinguishable is the turnover resulting from the pile-up, which completely obliterates the information in the innermost regions for 1E 1740.7−2942.

Looking at Fig. 4(a), where the surface brightness distributions between 2.5 and 3.5 keV are plotted, we can see the profile of 1E 1740.7−2942 quite significantly exceeding that of PKS 2155−302 between about 5 and 30 arcsec.

The amount by which 1E 1740.7−2942 exceeds PKS 2155−304 is dependent on a number of factors; seeking to minimize the effect of pile-up, as noted above, we have normalized the data sets at a radius of 4 arcsec. In Fig. 5 we plot the fractional halo intensity, defined as *halo/(source + halo)*, as a function of angular distance from 1E 1740.7−2942. The excess, at a level of 30–40 per cent (mean value 32 ± 7 per cent), is detected out to 40 arcsec from the core, in the lower (2.5–3.5 keV) energy band. In the higher energy band (4.5–5.5 keV) there is no significant excess, although the poor statistics means that the 3σ upper limit is only 30 per cent.

Based on Predehl & Schmitt (1995) we would expect a *total* fractional halo intensity (i.e. summed over all angles) of ∼50 per cent

[1]See http://asc.harvard.edu/ciao/caveats/psflib.html and http://cxc.harvard.edu/cal/Hrma/hrma/psf/psfwings/psfwings.html.

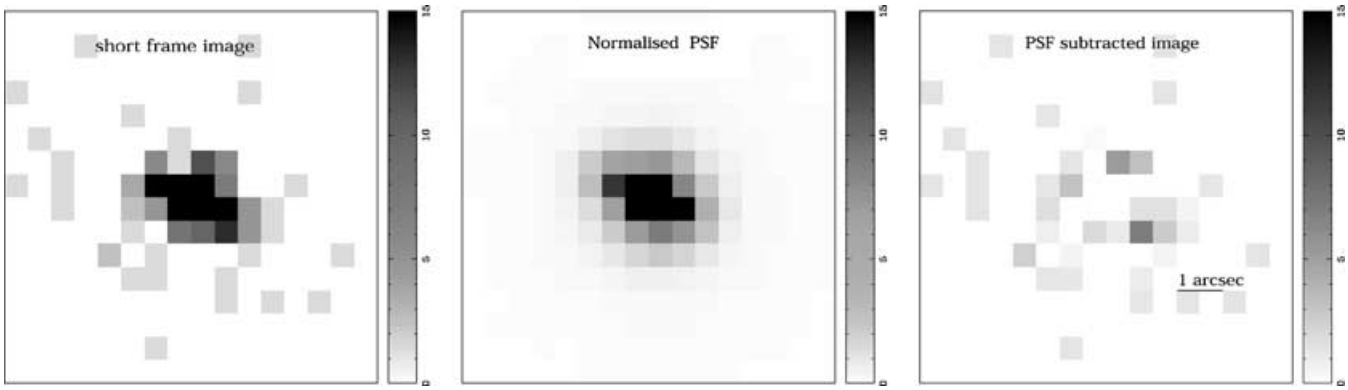

Figure 3. (Left panel) The zeroth-order *Chandra* HETGS observation of 1E 1740.7−2942 performed in 1999 with a short frame time (0.2 ks of net exposure, in order to avoid pile-up effects). (Centre panel) The *Chandra* PSF we calculated through an interpolation of library PSFs. Such a calculation has been made in order to reproduce what a point source observed by *Chandra* in the brightest point of the previous image and normalized to the same number of counts should look like. (Right panel) The PSF-subtracted short frame image. Fitting a MARX simulated PSF to the radial profile of the short frame image collapsed along and across the direction of the elongation, Cui et al. (2001) found evidence of an X-ray elongated feature roughly perpendicular to the radio jet axis. However, comparing the same image with the right *Chandra* PSF we do not confirm such an analysis; no elongated structure appears after the PSF subtraction from the whole image. The residuals in the right-hand panel result from the fact that the PSF, which is position-dependent as well as energy-dependent, has been calculated at 5.5 keV, where the short frame image reaches the highest number of counts.

at 3 keV and ∼20 per cent at 5 keV for such a large $N_{\rm H}$. However, uncertainties in the angular and energy dependence of both the pile-up and the PSF, as well as in the angular distribution of scattered photons, do not allow us to easily estimate this value. We do note, however, that the apparent weakness of the halo at 5 keV may suggest that most of the absorption is made locally at the source. Actually, such a possibility has already been proposed in previous works, where 1E 1740.7−2942 is supposed to be embedded in a dense molecular cloud (Bally & Leventhal 1991; Mirabel et al. 1991; Phillips et al. 1995; Yan & Dalgarno 1997). If there was dust scattering emission potentially associated with a local environment, *Chandra*, with its excellent angular resolution, should in principle be able to detect this, although it would require a much longer observing time.

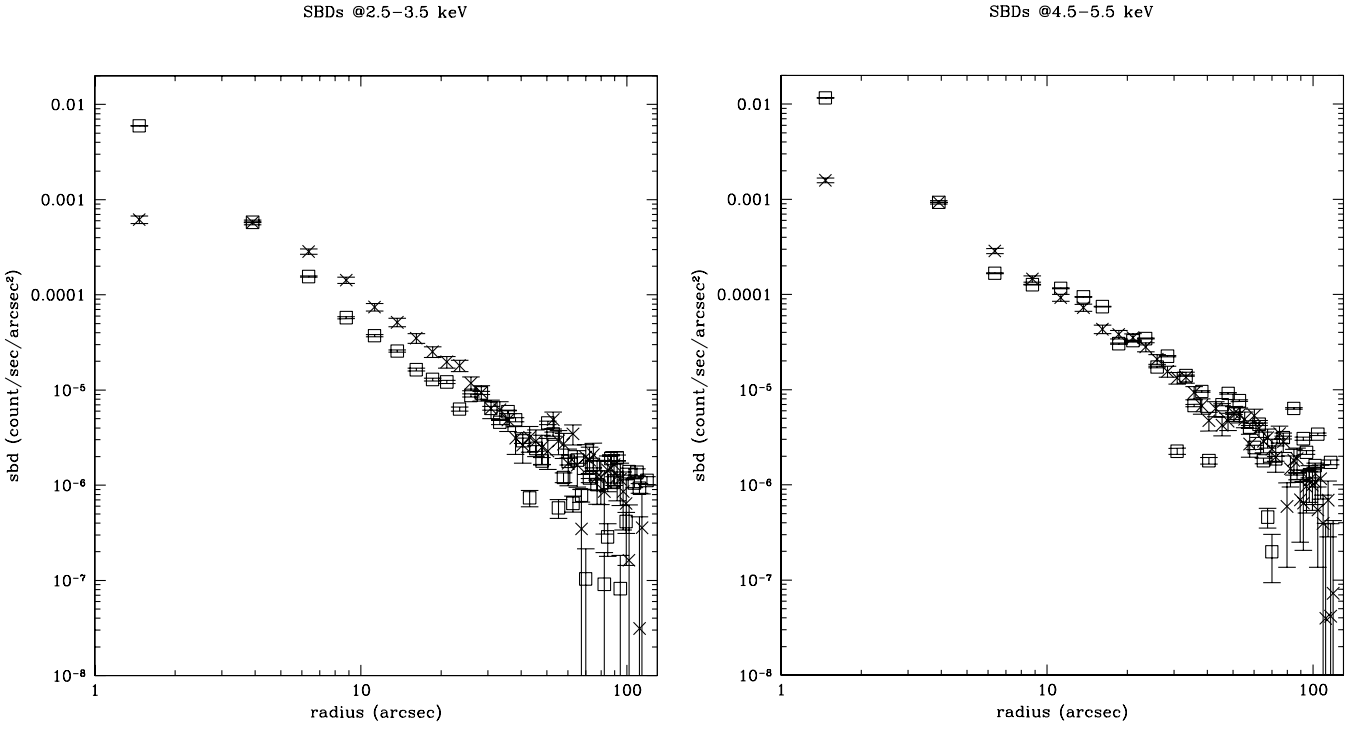

Figure 4. Surface brightness distributions of 1E 1740.7−2942 (crosses) in units of count s^{-1} $arcsec^{-2}$ versus arcsec compared with the unscattered X-ray point source PKS 2155−304 (squares) in two different energy bands: 2.5–3.5 keV and 5.5–6.5 keV (left and right panels, respectively). Well recognizable are the effects of the pile-up, which correspond to lost and undetected events up to a radius of about 2–3 arcsec. The profiles have been normalized to the surface brightness distribution value at about 4 arcsec, supposing that in this region the effects of the pile-up are almost negligible. The contribution of the X-ray halo is well recognizable in the softer band (bottom left panel).

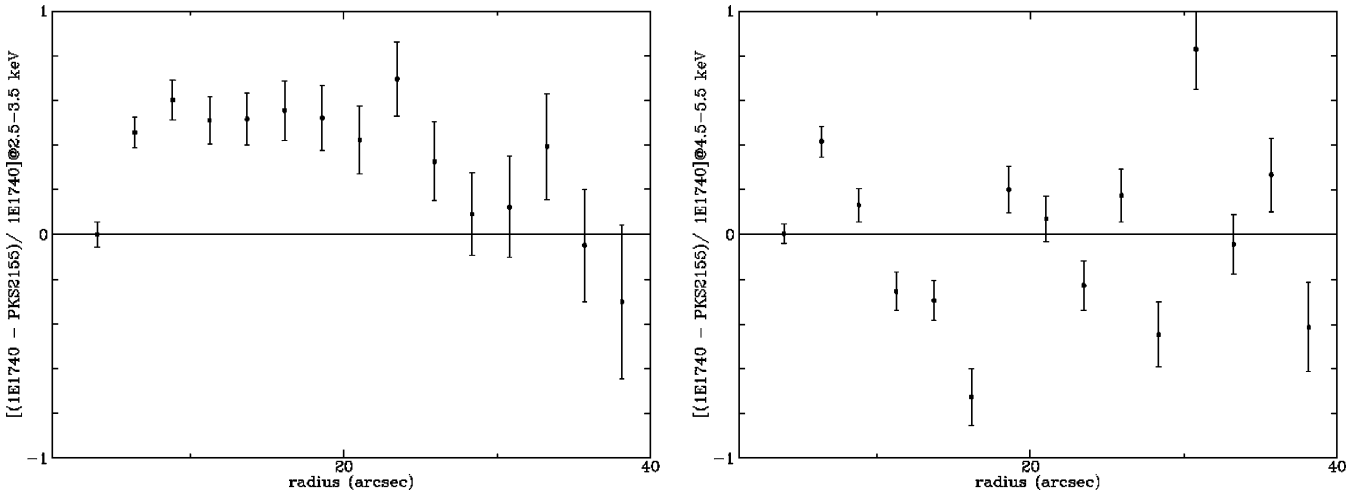

Figure 5. Halo fractional intensities, $I_{\rm frac}$, versus radius between (left panel) 2.5 and 3.5 keV and (right panel) 4.5 and 5.5 keV. In the softer band, the mean fraction of scattered X-ray photons within 40 arcsec is 32 ± 7 per cent. In the harder band, the mean fraction is -2 ± 10 per cent, which means that the 3σ upper limit is only 30 per cent.

Obviously our analysis is biased by several approximations. First of all, the severe pile-up effects make it necessary to choose a normalization factor between the source and PSF profiles. In addition, there is the choice of the PSF itself, which, being different from the proper calibrated *Chandra* PSF, certainly introduces errors resulting from, for instance, position dependence, different background level and so on.

4 CONSTRAINING B IN THE RADIO LOBES

1E 1740.7−2942 is associated with an unresolved, flat-spectrum radio core and two extended, optically thin radio lobes (Mirabel et al. 1992; Anantharamaiah et al. 1993). The high-energy electrons present in such lobes are expected to Comptonize the ambient photons and, as a result, should produce some high-energy X-ray emission. We have inspected our image for X-ray emission associated with the northern lobe (lobe 'B'), in order to place limits on any Comptonized component. Unfortunately, this lobe partially lies in the gap between the ACIS-I3 and I2 chips; however, after calculating the exposure maps we are still able to place a limit on the X-ray flux associated with the lobe. The net count rate in a circular region of radius 8 arcsec centred on lobe B is 2.0×10^{-3} count s^{-1}. We then ran a PIMMS simulation in order to evaluate the X-ray flux emerging from that region. We used the $N_{\rm H}$ column density obtained from the readout streak spectrum and we chose a power-law model with a photon index of 1.5, i.e. the typical slope resulting from single-scattering Comptonization. In this way, we were able to estimate a firm upper limit to the X-ray flux, which turned out to be $\leqslant 8.8 \times 10^{-14}$ erg cm^{-2} s^{-1}. Note that, at such an angular distance from the core, in fact, the contaminations to the X-ray emission from the PSF and dust scattering halo are far from being negligible; however, without a good model we are not able to do any better than this currently. We then evaluated the radio flux between 1 and 6 GHz assuming a spectral index of $\alpha = -0.9$ (using the conventional definition, $S_\nu \propto \nu^\alpha$), according to Mirabel et al. (1993), and a peak flux density of 0.27 mJy at 5 GHz (Anantharamaiah et al. 1993). In this way, we obtained a radio flux of $\sim 2 \times 10^{-16}$ erg cm^{-2} s^{-1}, giving a ratio $E_X/E_{\rm Radio} \leqslant 500$. This ratio constrains the ratio of photon to magnetic energy densities, $U_\gamma : U_B$, subject to the caveat of our rather limited spectral coverage and assuming isotropic emission in both bands. In the Galactic Centre region, the photon energy density has been recently estimated to be ~ 10 eV cm^{-3}, i.e. $\sim 2 \times 10^{-11}$ erg cm^{-3} (Strong, Moskalenko & Reimer 2000). Thus, our observations roughly constrain the magnetic field in the lobes to $B \geqslant 1$ μG. Given that the equipartition fields associated with the radio jets and lobes of X-ray binaries are typically estimated to be of the order of milligauss or more (see, for example, Spencer 1996), this is not surprising. Nevertheless, it does provide an entirely independent lower limit on the magnetic field in the lobes.

5 CONCLUSIONS

We have performed a detailed analysis of a 10-ks *Chandra* ACIS-I observation of the black hole candidate 1E 1740.7−2942. The conclusions of this work are as follows.

(i) We have utilized two approaches to measuring the X-ray spectrum without suffering the effects of pile-up, which are very strong in the core of our image. Using the readout streak, the 2–10 keV spectrum is well fitted by an absorbed power law with $\Gamma = 1.54^{+0.42}_{-0.37}$ and $N_{\rm H} = 11.8^{+2.3}_{-1.9} \times 10^{22}$ cm^{-2}. Using an annulus from 4 to 30 arcsec, providing more counts but potentially more prone to pile-up effects, we also fitted an absorbed power law, with $\Gamma = 1.42^{+0.14}_{-0.14}$ and $N_{\rm H} = 10.45^{+0.73}_{-0.70} \times 10^{22}$ cm^{-2} with χ^2/d.o.f. $= 430/331$. Both results are consistent, as expected, with a black hole low/hard state, and furthermore indicate that the annulus approach does not suffer too badly, if at all, from pile-up.

(ii) We do not confirm the presence of an elongated X-ray feature (about 3 arcsec) reported by Cui et al. (2001). Analysing the same data set, now public, we did not find evidence for any asymmetric X-ray structure within about 4 arcsec from the centre. On larger angular scales, there is no obvious asymmetry – in deeper images from our new data – to several arcmin.

(iii) We have calculated and compared the surface brightness distributions of 1E 1740.7−2942 to those of an unscattered X-ray source in different energy bands. Despite complications because of pile-up effects and uncertain PSFs, which make the comparison between the profiles very sensitive to the normalization factor, we found clear evidence for scattered X-rays in the energy range 2.5–3.5 keV at an angular separation $\lesssim$40 arcsec from the core. At higher energies and/or larger angular separations, the scattering halo is not clearly detectable.

(iv) We have provided an upper limit on the ratio between X-ray and radio fluxes in the region that corresponds to the hotspot at the end of the northern radio jet emitted by 1E 1740.7−2942, from which we can crudely constrain $B_{\rm lobe} \geqslant 1\mu$G.

Even though 1E 1740.7−2942 is, in principle, an ideal candidate for the study of X-ray scattering haloes because of its huge column density, which is proportional to the amount of dust grains along the line of sight, such an investigation is complicated by the fact that the source is almost completely absorbed below about 3 keV. Theoretically, the optical depth due to scattering scales as E^{-2}, making the softer, i.e. *the absorbed*, band more suitable for investigating X-ray haloes. This demonstrates that there is a limit to the study of haloes that can be performed with *Chandra* for such strongly absorbed sources such as 1E 1740.7−2942, because the absorbing $N_{\rm H}$ column is also proportional to the amount of dust scattering. Comparing the halo brightness with X-ray absorption would allow us to directly quantify the amount and the density of that molecular cloud; a detailed analysis of the relation between halo and scattering dust properties is, however, beyond the aim of this paper.

Finally, we would like to stress that, in order to correctly compare the radial profile of a source, which is supposed to show an X-ray scattering halo or other extended features, with that of a point-like source, it will be necessary to carry out a detailed comparison between simulated and measured PSF wings profiles. However, until a complete calibration of the PSF wings is available, using real observations as a template remains our best option.

ACKNOWLEDGMENTS

We would like to thank Michiel van der Klis for useful comments, and the anonymous referee for his/her constructive criticism which helped significantly to improve the paper.

REFERENCES

Anantharamaiah K. R., Dwarakanath K. S., Morris D., Goss W. M., Radhakrishnan V., 1993, ApJ, 410, 110
Bally J., Leventhal M., 1991, Nat, 353, 234
Bouchet L. et al., 1991, ApJ, 383, L45
Churazov E., Gilfanov M., Sunyaev R., 1996, ApJ, 464, L71
Cui W. et al., 2001, ApJ, 548, 394
Djorgovski S. G., Thompson D., Mazzarella J., Klemola A., 1992, IAU Circ. 5596
Eikenberry S. S., Fischer W. J., Egami E., Djorgovski S. G., 2001, ApJ, 556, 1, 1
Garmire G. P., 1997, BAAS, 190, 34.04
Jung G. V. et al., 1995, A&A, 295, L23
Liang E., 1993, in Friedlander M., Gehrels N., Macomb D., eds, AIP Conf. Proc. Vol. 280, Compton Gamma Ray Observatory. Am. Inst. Phys., New York, p. 418
Liang E., Nolan P., 1984, Space Sci. Rev., 38, 353
Main D. S., Smith D. M., Heindl W. A., Swank J., Leventhal M., Mirabel I. F., Rodriguez L. F., 1999, ApJ, 525, 901
Marti J., Mirabel I. F., Chaty S., Rodriguez L. F., 2000, A&A, 363, 184
Mereghetti S., Caraveo P., Bignami G., Belloni T., 1992, A&A, 259, 205
Mirabel I. F., Duc P. A., 1992, IAU Circ. 5655
Mirabel I. F., Morris M., Wink J., Paul J., Cordier B., 1991, A&A, 251, L43
Mirabel I. F., Rodriguez L., Cordier B., Paul J., Lebrun F., 1992, Nat, 358, 215
Mirabel I. F., Rodriguez L. F., Cordier B., Paul J., Lebrun F., 1993, A&AS, 97, 193
Phillips J. A., Joseph T., Lazio W., 1995, ApJ, 442, L37
Predehl P., Schmitt J. H. M. M., 1995, A&A, 293, 889
Predehl P., Burwitz V., Paerels F., Trümper J., 2000, A&A, 357, L25
Prince T., Skinner G. K., 1991, IAU Circ. 5252
Sakano M., Imanishi K., Tsujimoto M., Koyama K., Maeda Y., 1999, ApJ, 520, 316
Sheth S., Liang E., Luo C., Murakami T., 1996, ApJ, 468, 755
Smith D. M., Heindl W. A., Swank J. H., 2001, American Astronomical Society Meeting, 199, 108.01
Spencer R. E., 1996, in Taylor A. R., Paredes J. M., eds, ASP Conf. Ser. Vol. 93, Radio emission from the stars and the Sun. Astron. Soc. Pac., San Francisco, p. 252
Strong A. W., Moskalenko I. V., Reimer O., 2000, ApJ, 537, 763
Sunyaev R. et al., 1991a, in Durouchoux P., Prantzos N. eds, AIP Conf. Proc. Vol. 232, gamma Ray Line Astrophysics. Am. Inst. Phys., New York, p. 29
Sunyaev R. et al., 1991b, ApJ, 383, L49
Yan M., Dalgarno A., 1997, ApJ, 481, 296

This paper has been typeset from a TEX/LATEX file prepared by the author.